

A novel ribosomal protein S6 kinase 2 inhibitor attenuates the malignant phenotype of cutaneous malignant melanoma cells by inducing cell cycle arrest and apoptosis

Yayun Li^{a,b,c}, Pian Yu^{a,b,c}, Jing Long^{a,b,c}, Ling Tang^{a,b,c}, Xu Zhang^{a,b,c}, Zhe Zhou^{a,b,c}, DongSheng Cao^d, Juan Su^{a,b,c}, Xiang Chen^{a,b,c}, and Cong Peng^{a,b,c,*}

^aDepartment of Dermatology, Hunan Engineering Research Center of Skin Health and Disease, Hunan Key Laboratory of Skin Cancer and Psoriasis, Xiangya Clinical Research Center for Cancer Immunotherapy, Xiangya Hospital, Central South University, Changsha, Hunan, China; ^bNational Engineering Research Center of Personalized Diagnostic and Therapeutic Technology, Central South University, Changsha, Hunan, China; ^cNational Clinical Research Center for Geriatric Disorders, Xiangya Hospital, Central South University, Changsha, Hunan, China; ^dHunan Key Laboratory of Processed Food for Special Medical Purpose, Central South University of Forestry and Technology, Hunan, China

ABSTRACT

Malignant melanoma (MM) is a highly life-threatening tumor causing the majority of the cutaneous cancer-related deaths. Previously, ribosomal protein S6 kinase 2 (RSK2), the downstream effector of the MAPK pathway, represents a therapeutic target in melanoma. AE007 is discovered as a targeted RSK2 inhibitor, and subsequent results showed that AE007 inhibits RSK2 by directly binding to its protein kinase domain. AE007 causes cell cycle arrest and cellular apoptosis, thereby dramatically inhibiting proliferation, migration, and invasion of melanoma cells. Nevertheless, melanocytes and keratinocytes are not affected by this compound. In addition, suppression of RSK2 abrogates the inhibitory effect of AE007 on melanoma cell proliferation. AE007 treatment significantly inhibits the expression of Cyclin D1, Cyclin B1, CDK2, and Bcl-2, while raises the cleavage of PARP. Moreover, RNA sequencing results show that AE007 treatment can affect the genes expression profile, including the expression of cell cycle and DNA replication genes. In conclusion, AE007 is a promising melanoma therapeutic agent by targeting RSK2.

ARTICLE HISTORY

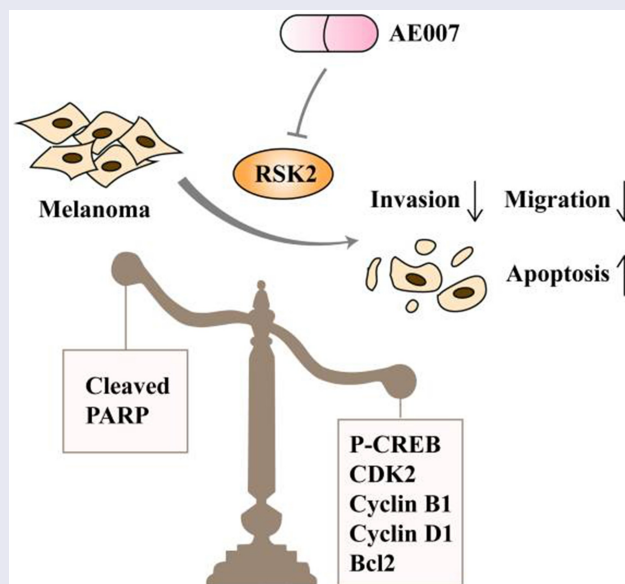
Received 18 February 2022

Revised 13 May 2022

Accepted 17 May 2022

KEYWORDS

Melanoma; RSK2; AE007; cell cycle arrest; apoptosis



*CONTACT Cong Peng  pengcongxy@csu.edu.cn  Department of Dermatology, Hunan Engineering Research Center of Skin Health and Disease, Hunan Key Laboratory of Skin Cancer and Psoriasis, Xiangya Hospital, Central South University, Changsha, Hunan, China; Xiang Chen  chenxiangck@126.com  Department of Dermatology, Hunan Engineering Research Center of Skin Health and Disease, Hunan Key Laboratory of Skin Cancer and Psoriasis, Xiangya Clinical Research Center for Cancer Immunotherapy, Xiangya Hospital, Central South University, Changsha, Hunan, China  Supplemental data for this article can be accessed online at <https://doi.org/10.1080/21655979.2022.2080364>

Highlights

- Identification of AE007 as a novel RSK2 inhibitor.
- AE007 inhibit melanoma progression in vitro and in vivo.
- AE007 causes cycle arrest and apoptosis in melanoma.

Introduction

Malignant melanoma is one of the most lethal disease of cutaneous cancers [1]. Over the past years, several novel systematic therapies including immune-checkpoint inhibitors, targeted therapies, or the combination of both, have contributed to improve survival rate of melanoma patients [2]. However, long-term clinical efficacy is often compromised because of innate or acquired resistance and dose-limiting toxicity [3]. Therefore, it is necessary to clarify the disease pathogenesis and find new therapeutic drugs with low toxicity for melanoma treatment.

There are numerous genomic mutations in melanoma patients. The mainly mutation genes include *BRAF*, *NRAS*, *KIT* and are associated with the treatment and prognosis [4]. Mutations of these genes usually lead to abnormal activation of RAS/RAF/MEK signaling pathway [5]. Therefore, targeting the signaling pathways is promising treatment for advanced melanoma patients. RSK2 is an important downstream effector of the MAPK pathway that controls proliferation, transformation, cell cycle progression, and apoptosis [6]. RSK2 phosphorylates various nuclear proteins including c-Fos [7], p53 [8], cyclic AMP responsive element-binding (CREB) [9], activating transcription factor 4 (ATF4) [10], nuclear factor of activated T cells 3 (NFAT3) [11]. RSK2 is also dysregulated in several malignancies, such as breast [12], lung [13], and prostate cancers [14], and malignant melanoma [15]. Previously, we found that knockdown of RSK2 expression in melanoma cells induces autophagy and inhibits its proliferation, migration and invasion. More importantly, RSK2 inhibition significantly attenuated BRAF inhibitor resistant melanoma cells malignant phenotype. These findings highlighted the significance of targeting RSK2 in melanoma.

Many efforts have been made in discovering RSK2 inhibitors. SL0101, isolated from the tropical plant *Forsteronia refracta*, was identified as the first small-molecule, RSK-specific inhibitor. SL0101 inhibits proliferation of the human breast cancer cell line MCF-7, but not alters proliferation of a normal human breast cell line MCF-10A [16]. Moreover, BI-D1870 and FMK were discovered as a specific inhibitor of RSK2 in non-tumor cells [17,18]. LJH685 functions as RSK2 inhibitor in MAPK-driven cancers including melanoma, while high EC50 limits its clinic use [19]. Carnosol were reported to suppresses the growth of gastric cancer and melanoma by targeting RSK2 [20,21], and could be a promising treatment for melanoma.

Whether there exists a novel RSK2 inhibitor which functions better than Carnosol in melanoma needs to be further clarified. Here, we used an in-silico strategy that combined ligand-based and structure-based virtual screening to identify the novel RSK2 inhibitor (AE007). We further observed that AE007 significantly inhibited the melanoma progression in vitro and in vivo via inducing cell cycle arrest and apoptosis. More important, the inhibitory effect of AE007 on melanoma was stronger than that of Carnosol. Altogether, we identify a novel RSK2 inhibitor which will provide a novel strategy for melanoma treatment in clinic.

Materials and methods

Virtual screening

An in-silico strategy was proposed for identifying RSK2 inhibitors from the SPECS database. On the basis of existing RSK2 bioactivity data, three QSAR models were developed, namely two-dimensional MOE descriptors (MOE2D), molecular fragment descriptors (MACCS), and 2-point pharmacophore descriptors (CATS). These models were employed for considering the validation results to determine their capability of conducting the classification of RSK2 inhibitors. Subsequently, the validation results of these models showed that they can effectively classify RSK2 inhibitors. After application of a series of selection criteria and ADMET analysis, compounds were performed for SPR binding assays and its inhibitory activities

on melanoma, based on their IC50 values, as previously described [22].

Cell culture

The American Type Culture Collection (ATCC; Manassas, VA) provided the human malignant melanoma cell lines SK-MEL-5, SK-MEL-28, A375, B16F10, human melanocyte cell line (PIG1), normal human epidermal keratinocytes (HaCaT), and human embryonic kidney cell line (HEK293T). High-glucose Dulbecco's modified Eagle's medium (DMEM; Biological Industries, Israel), RPMI 1640 medium supplemented with 10% fetal bovine serum (FBS; Biological Industries, Israel), or medium 254 (Gibco; Thermo Fisher Scientific; USA) was used for these cell lines at 37°C in 5% CO₂ humidified incubators according to the protocol. All cell lines were routinely tested for mycoplasma to ensure no contamination.

Cell viability

A total of 2–4 × 10³ cells per well were seeded into 96-well plates and treated with AE007 or DMSO (100* μ L/well) for 1-, 2- and 3-day period. The four different time periods were involved for considering treatment effect during different periods for a comprehensive understanding. Then, the CCK-8 reagent (Selleck, USA) was added, followed by incubation for 2–3 hours at 37°C. Using a microplate reader, the optical density (OD) at 450 nm was determined (Thermo Fisher Scientific, USA). In addition, four replicates per group were established. Cell viability curves were generated and half-maximal inhibitory concentrations (IC50) were determined using GraphPad Prism software (San Diego, Calif).

Colony formation assay

We plated cells in 6-well plates at 0.5–1 × 10³ density overnight (TC20 Automated Cell Counter, Bio-Rad). AE007 or DMSO (vehicle, 1:5000) were then added to the cells for 48 hours. A complete growth medium was used to culture the cells for approximately 14 days until colonies began to appear. Crystal violet (0.5%, Beyotime,

China) and 4% paraformaldehyde were applied to the colonies at room temperature.

Wound curative assay

Cells were seeded until they reached 90–95% confluence. Then cells were treated with DMSO (vehicle) or different concentrations of AE007 after scratching the cell layer with a 10 μ L pipette tip. Images were taken under microscope at the indicated time points after scraping. The wound surface area was quantified using Image J.

Invasion assay

The membranes of Boyden chamber inserts (Corning, USA) were precoated with Matrigel diluted 1:4 in a serum-free medium. AE007 was then added to a 10% FBS medium containing the same concentration of AE007 in the lower chambers after the Matrigel had polymerized. Cells were seeded in the upper chambers once the Matrigel had polymerized. The cells were allowed to invade the serum-containing medium through the Matrigel for 24–48 hours in the incubator. A crystal violet stain was applied after the cells were fixed in 4% formalin and the inserts were dismantled. The migrated cells were examined by microscope.

Apoptosis and cell cycle analyses

DMSO (vehicle, 1:5000) or various concentrations of AE007 were applied to the cells for 48 hours. Apoptosis status was evaluated with flow cytometry (Becton, Dickinson Company, USA), utilizing Annexin V-FITC/PI Apoptosis Detection Kits (BD Biosciences, New Jersey, USA), and data analysis were performed with FlowJo software. To study cell cycle, ethanol-fixed cells (Beyotime, China) were fixed at 4°C overnight and stained in propidium iodide (PI) at room temperature for 30 minutes. Flow cytometric measurements were conducted for cell cycle distribution, and data evaluation was conducted using ModFit software.

Western blotting

The cells were incubated on ice for 30 minutes with RIPA lysis buffer (Beyotime, China) containing protease inhibitors and phosphatase inhibitors (Selleck, USA). After centrifuging at 13,000 rpm for 20 minutes, the total protein concentration was determined using a BCA protein assay kit (Beyotime, China). The temperature during the whole process was kept at 4°C. After mixing the cell lysate with loading buffer, the protein mixture was denatured at 95°C for 10 minutes, then separated by electrophoresis on an SDS-polyacrylamide gel and electrotransferred onto a PVDF membrane (Millipore, USA). After blocking the PVDF membrane for 1–2 h at 25°C with Tris-buffered saline/0.1% Tween 20 (TBST) containing 5% skim milk, the membrane was rinsed three times with TBST buffer, and the primary antibody was incubated at 4°C overnight. Horseradish peroxidase-conjugated anti-rabbit/anti-mouse IgG antibodies were added to the membrane as secondary antibodies at 25°C for 1–2 h. The PVDF membrane was then developed using an ECL reagent (NCM Biotech, China). The antibodies used were as follows: RSK2 (Cell Signaling Technology, MA, USA, #5528T, 1:1000), p-CREB (Cell Signaling Technology, MA, USA, #9198S, 1:1000), CREB (Cell Signaling Technology, MA, USA, #9197S, 1:1000), Bcl-2 (Proteintech, CHI, USA, #12789-1-AP, 1:1000), PARP (Cell Signaling Technology, MA, USA, #9532S, 1:1000), CDK2 (Proteintech, MA, USA, #10122-1-AP, 1:1000), cyclin D1 (Cell Signaling Technology, MA, USA, #55506S, 1:1000), cyclin B1 (Santa Cruz Biotechnology, TX, USA, #sc-245, 1:1000), p-IκBα (Cell Signaling Technology, MA, USA, #5209S, 1:1000), GAPDH (Proteintech, MA, USA, #60004-1-Ig, 1:1000).

Pull down assay

Cell lysates were incubated with agarose 4B beads crosslinked to AE007, as described previously [23].

Purification of IκBα proteins and in vitro kinase assay

(His) 6-labeled IκBα protein was purified by ultrasound from BL21 (DE3) cells using a preestablished method in our laboratory [23].

Quantitative real-time PCR analysis

Cell samples were lysed with TRIzol reagent (Invitrogen, CA, USA). The RNA was isolated using the phenol/chloroform method and purified according to the instructions. SuperScript III First-Strand Synthesis System (Invitrogen, California, USA) was used for reverse transcription. Real-time PCR was performed with SYBR Green Master Mix (CWBIO, Jiangsu, China) in Applied Biosystems QuantStudio™ 3 Real-Time PCR System (Thermo Fisher Scientific, MA, USA). Gene expressions were normalized to GAPDH expression. Data of RNA-seq can be found in the NCBI's Sequence Read Archive (SRA) database (BioProject ID: PRJNA792212, Submission ID: SUB10830073). The Real-Time PCR primers are in **Table S1**.

Plasmids and transfection of cells

Plasmids *RSK2* (NM_004586.3) and *IκBα* (NM_020529.3) were constructed in pLVX-IRES-Puro vector (Clontech). Transfection of 293 T cells was carried out with Turbofect Transfection Reagent (Thermo Scientific) for 16 hours in order to select for other genes. After 48 hours and 72 hours, lentiviral particles were collected in the supernatant and used for transduction of melanoma cells with 2 μg/mL polybrene (Sigma). In a medium containing 2 μg/mL puromycin, stable cell lines were selected after 24 h. Western blotting was conducted for verification.

Xenograft mouse model

The animal use protocol listed below has been reviewed and approved by the Ethics Committee of Xiangya Hospital (Central South University, China). The guideline of animal experiment is required to minimize suffering and improve welfare of animals in research. Three groups of mice were assigned at random, including the solvent group (vehicle), AE007 30 mg/kg group, and AE007 60 mg/kg group (10 mice in each group), as previously described [24].

Immunohistochemistry

A primary anti-Ki67 (Abcam, Cambridge, UK, #AB16667, 1:300) was incubated by tissue sections overnight at 4°C in a humidified environment. The immunohistochemical experiment was performed as described previously. Images were photographed using microscope and quantified by Image J [25].

RNA-seq analysis

Total RNA from SK-MEL-28 were used for RNA-seq analysis. Library was constructed and validated on the Agilent Technologies 2100 bioanalyzer. RNA-seq were performed on a BGISEQ500 platform (Beijing Genomic Institution, BGI). Differential expression genes were defined with an adjusted p value of \log_2 -Ratio ≥ 1 and false discovery rate (FDR) ≤ 0.001 .

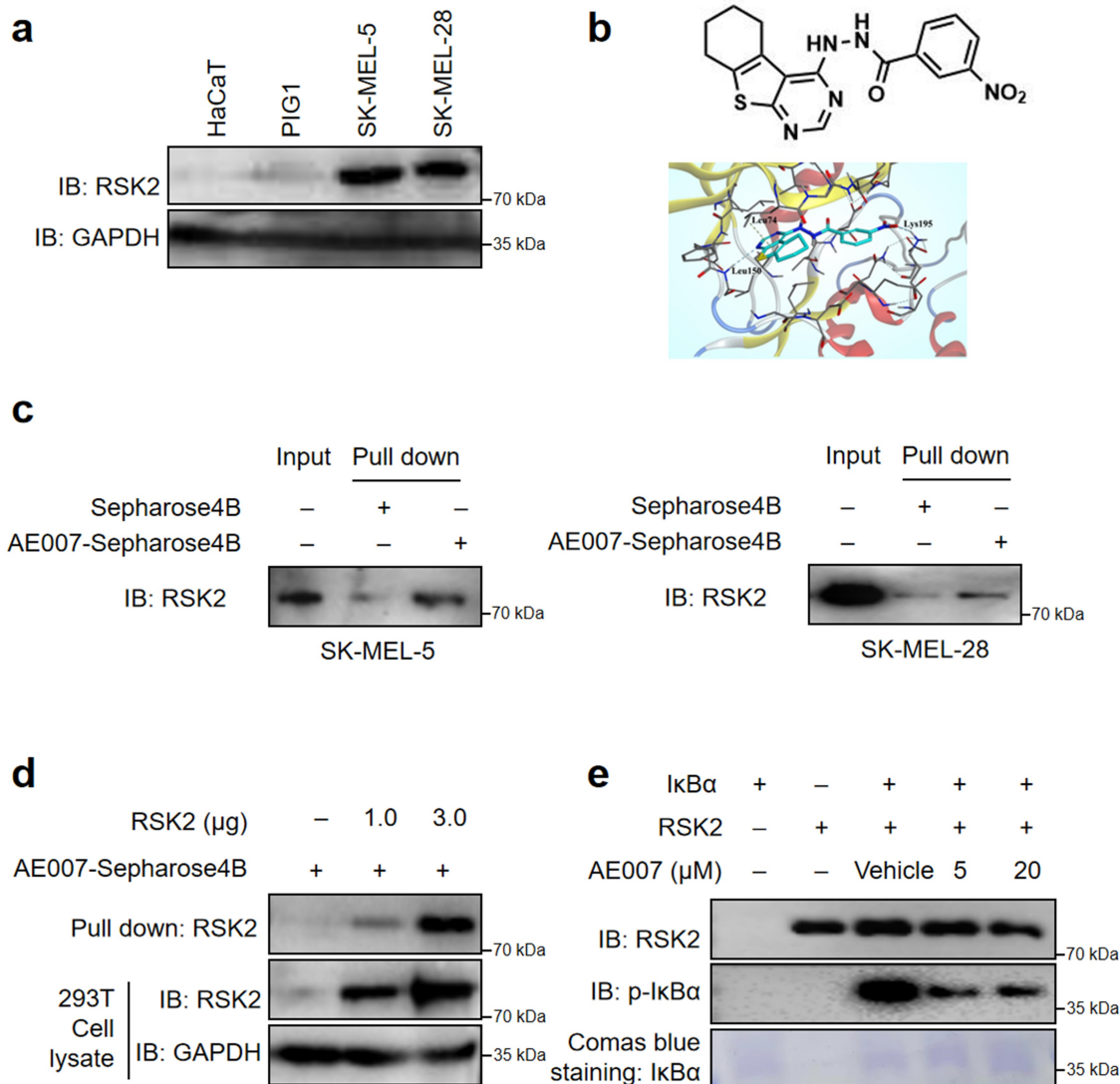


Figure 1. Identification of AE007 as a new RSK2 inhibitor. **(a)** The expression of RSK2 in HaCaT, PIG1, SK-MEL5 and SK-MEL-28. **(b)** Structure of AE007. The interaction between AE007 and RSK2 at three residues, Leu74, Leu150 and Lys195. **(c)** Immunoblot analysis of cell lysates from melanoma subjected to a pull-down assay using an anti-RSK2 antibody. The data represent three separate experiments. **(d)** Lysates of 293 T cells transfected with 1 μ g and 3 μ g of the RSK2 plasmid were collected and subjected to a pull-down assay. Immunoblotting was performed with antibodies against RSK2 and GAPDH. **(e)** In vitro kinase assays of RSK2 activity were conducted after treatment with AE007 at 5 μ M and 20 μ M. An immunoblot analysis of reaction mixtures was performed using antibodies against RSK2, p-IkB α (S32), and IkB α . The results represent three independent experiments.

Statistical analysis

GraphPad Prism was used for statistical analysis. Results are representative of three independent experiments and data were presented as mean \pm standard deviations. Two-tailed unpaired student's t test was used for comparisons between two groups. One-way ANOVA analysis was used for comparisons between multiple groups. Nonparametric tests were applied if the data are not normally distributed. Values of $p < 0.05$ are considered significant.

Results

AE007 binds directly to RSK2 and inhibits its protein kinase activity

Considering its overexpression and functional diversity of RSK2 in melanoma (Figure 1a), targeting RSK2 may provide a strategy for the treatment of melanoma. To identify the optimal drugs targeting RSK2, 28 compounds targeting RSK2 were selected by using an in-silico strategy that combined ligand-based and structure-based virtual screening (VS). AE007 was identified as the most effective drug in inhibiting melanoma viability (Figure 1b, Figure S1a). To verify whether AE007 can directly bind to RSK2, we collected melanoma cell lysates and cultured them with AE007-Sepharose 4B beads. The results showed that RSK2 binds exclusively to the AE007-Sepharose 4B bead complex (Figure 1c). Then, serially increasing concentrations of the RSK2 plasmid were transfected into HEK293T cells. The collected cell lysate was combined with AE007-Sepharose 4B beads after a pull-down assay. Interestingly, AE007 bound to RSK2 in a dose-dependent manner (Figure 1d). The in vitro kinase assay assessment was conducted to detect the effect of AE007 on RSK2 kinase activity. I κ B α was considered to be a substrate of RSK2 and was used to indicate the activity of RSK2 in our experiments. As shown in Figure 1e, AE007 inhibited I κ B α phosphorylation in a dose-dependent manner, indicating that RSK2 activity was blocked by AE007. These findings suggested that AE007 binds directly to RSK2 and inhibits its protein kinase activity.

AE007 inhibits melanoma cell growth

We next explored the effect caused by AE007 on melanoma cell growth. According to Figure 2a, the viability of melanoma cells was significantly inhibited after AE007 treatment in a dose- and time-dependent manner. However, AE007 had obvious selective cytotoxicity to PIG1 and HaCaT cells (Figure 2b). Moreover, inhibition of RSK2 activity attenuates the inhibitory effect of AE007 on the viability of melanoma cells (Figure S1b). As a result of 48 hours of AE007 treatment, the IC₅₀ values in A375, SK-MEL-5, and SK-MEL-28 cells were 7.152 μ M, 7.079 μ M, and 9.050 μ M, respectively (Figure 2c). We also tested the effect of a commercial RSK2 inhibitor Carnosol, and the IC₅₀ values of A375, SK-MEL-5, and SK-MEL-28 are 36.40 μ M, 38.20 μ M, and 40.41 μ M, respectively (Figure 2c). These results indicated that AE007 had a stronger inhibitory effect on melanoma cells than Carnosol. AE007 also inhibited plate colony formation of melanoma cells in a dose-dependent manner (Figure 2d-e). These findings suggested that AE007 was capable of suppressing the proliferation of melanoma cells in vitro. A xenograft model of melanoma in nude mice was created to determine AE007 effect in vivo on melanoma cell proliferation. The melanoma cells growth in nude mice was significantly inhibited at both low and high doses of AE007, compared with control group, without affecting the body weight, indicating the compound's minimal toxicity in mice (Figures 4a-b). Moreover, we also tested Ki67 expression in paraffin-embedded mice tumor tissues and found that Ki67 staining was inhibited in xenograft model mice after AE007 treatment, suggesting that AE007 inhibits melanoma cell growth in vivo (Figure 4c-d).

AE007 inhibits melanoma cell invasion and migration

Transwell assay and wound-healing assay were conducted to assess the effect of AE007 on cell migration and invasion. The number of migratory and invasive cells were significantly blocked with dosage- and time-dependent manner in melanoma cells (Figure 3a-d). We also investigated the effect of AE007 on pulmonary metastasis of B16F10 cells

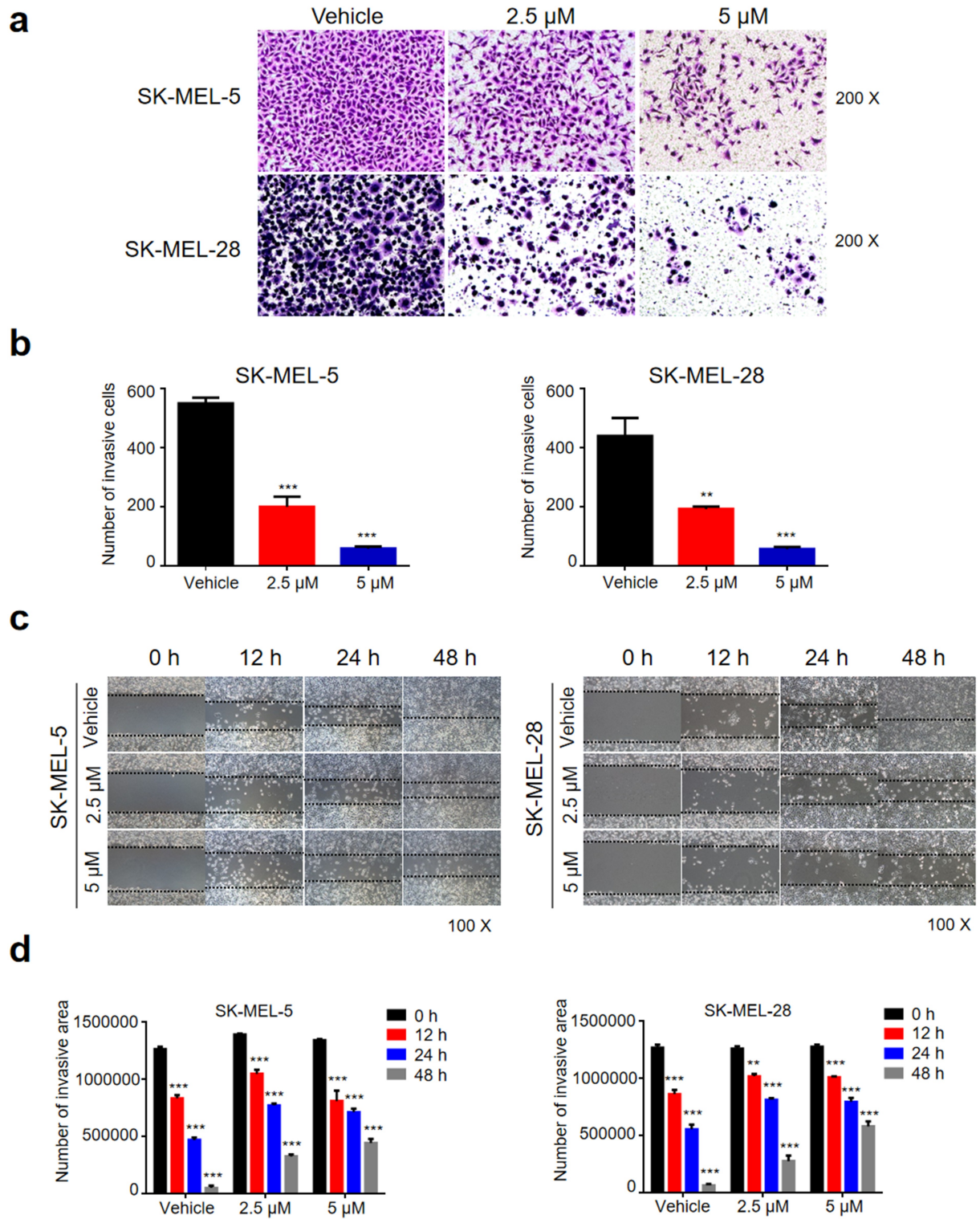


Figure 3. AE007 inhibits melanoma cell invasiveness and metastasis in vitro. **(a)** Transwell assays of melanoma cells treated with vehicle, AE007 at 2.5 μM and 5 μM for 24 h. **(b)** Quantification of transwell assay. **(c)** Wound healing assays of melanoma cells treated with vehicle, AE007 at 2.5 μM and 5 μM . Images (at 40x magnification) were acquired in the indicated time point. **(d)** Quantification of wound healing assay. One-way ANOVA analysis were performed in **b** and **d**. **, $P < 0.01$; ***, $P < 0.001$.

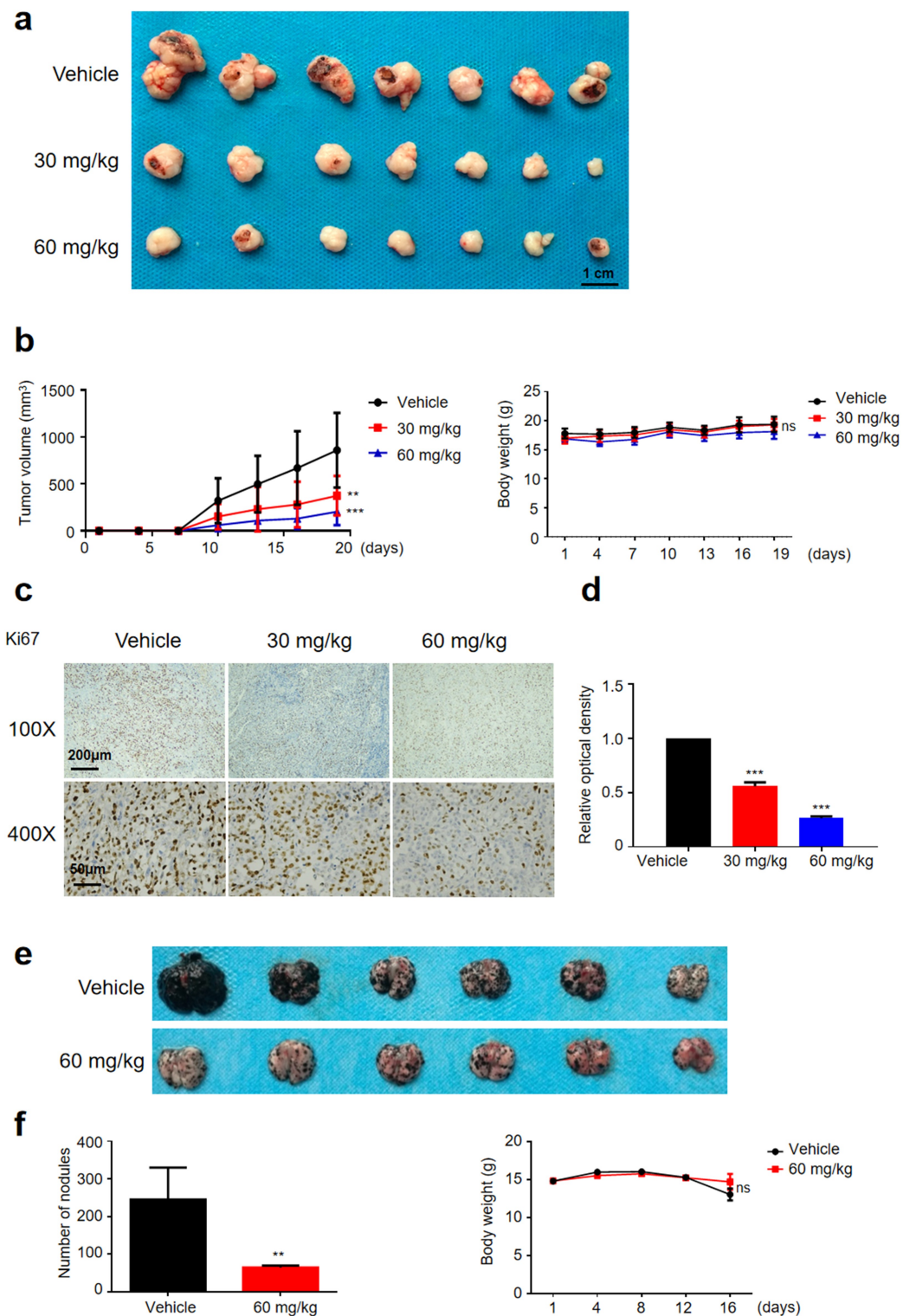


Figure 4. AE007 suppresses melanoma cell growth and metastasis in vivo. **(a).** Picture of the sectioned tumors. **(b).** Tumor volume and body weight in the indicated groups. **(c).** Ki67 staining by IHC of the sectioned tumors to identify tumor cell proliferation in the indicated groups. **(d).** Quantification of Ki67 staining. **(e).** Picture of metastatic nodules in lung. **(f).** Number of metastatic nodules in lung (left panel) and the body weight (right panel) in the indicated groups. P values were calculated using Brown-Forsythe and Welch ANOVA test in **b**, and Mann-Whitney test in **f**. **, $P < 0.01$; ***, $P < 0.001$.

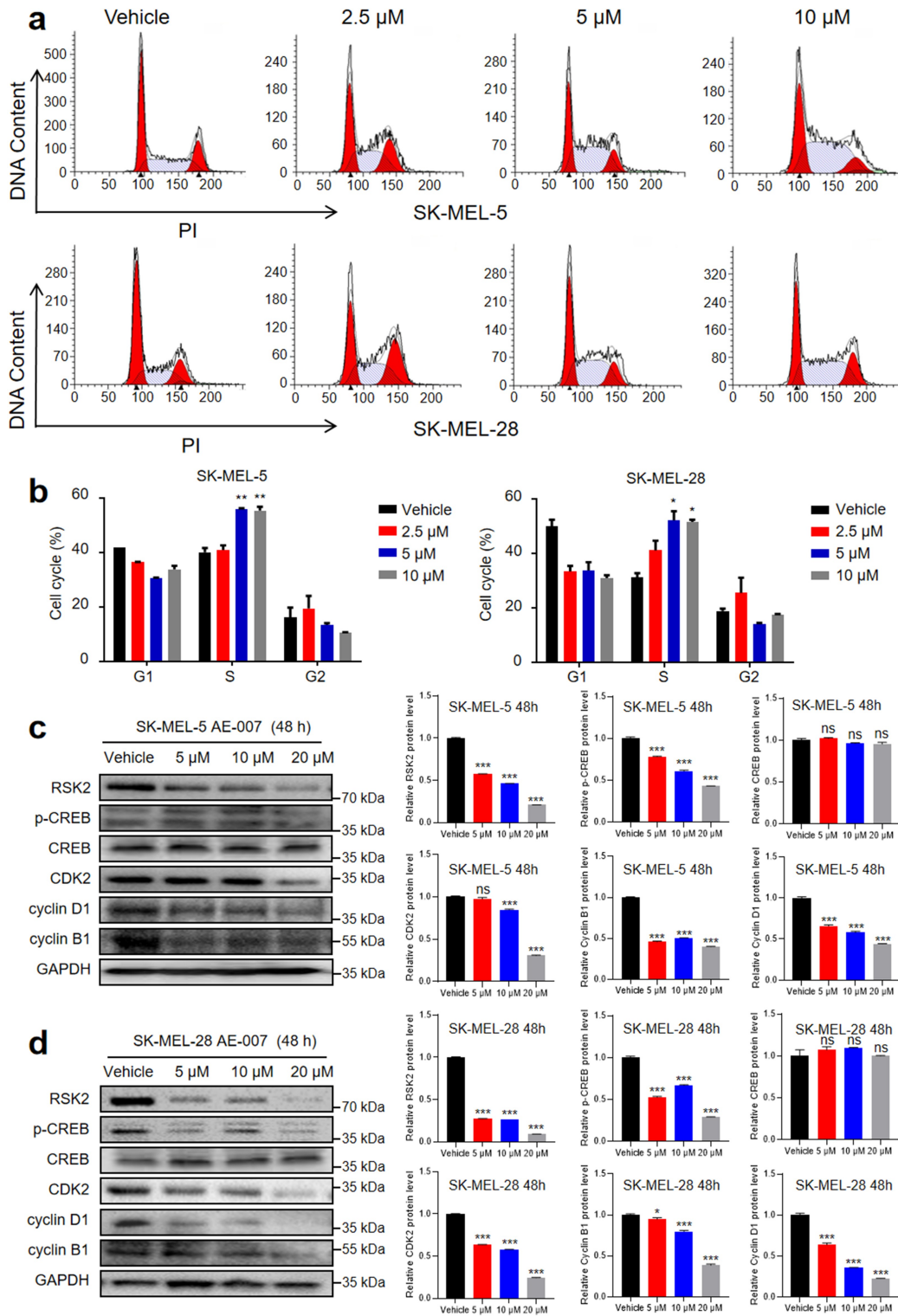


Figure 5. AE007 induces S-phase arrest and apoptosis in melanoma cells. **(a)** Cell cycle analysis of SK-MEL-5 (upper panel) and SK-MEL-28 (lower panel) cells treated with increasing concentrations of AE007 for 48 h. A flow cytometry analysis of the cell cycle distribution was performed. **(b)** Quantification of cell cycle. **(c)** SK-MEL-5 cells were treated with vehicle, AE007 at 5 μ M, 10 μ M, and 20 μ M. Immunoblotting was performed with antibodies against RSK2, p-CREB, CDK2, cyclin B1, cyclin D1, and GAPDH. **(d)** SK-MEL-28 cells were treated with vehicle, AE007 at 5 μ M, 10 μ M, and 20 μ M. Immunoblotting was performed with antibodies against RSK2, p-CREB, CDK2, cyclin B1, cyclin D1, and GAPDH. One-way ANOVA analysis were performed in **b**, **c** and **d**. *, $P < 0.05$; **, $P < 0.01$; ***, $P < 0.001$; ns, no significance.

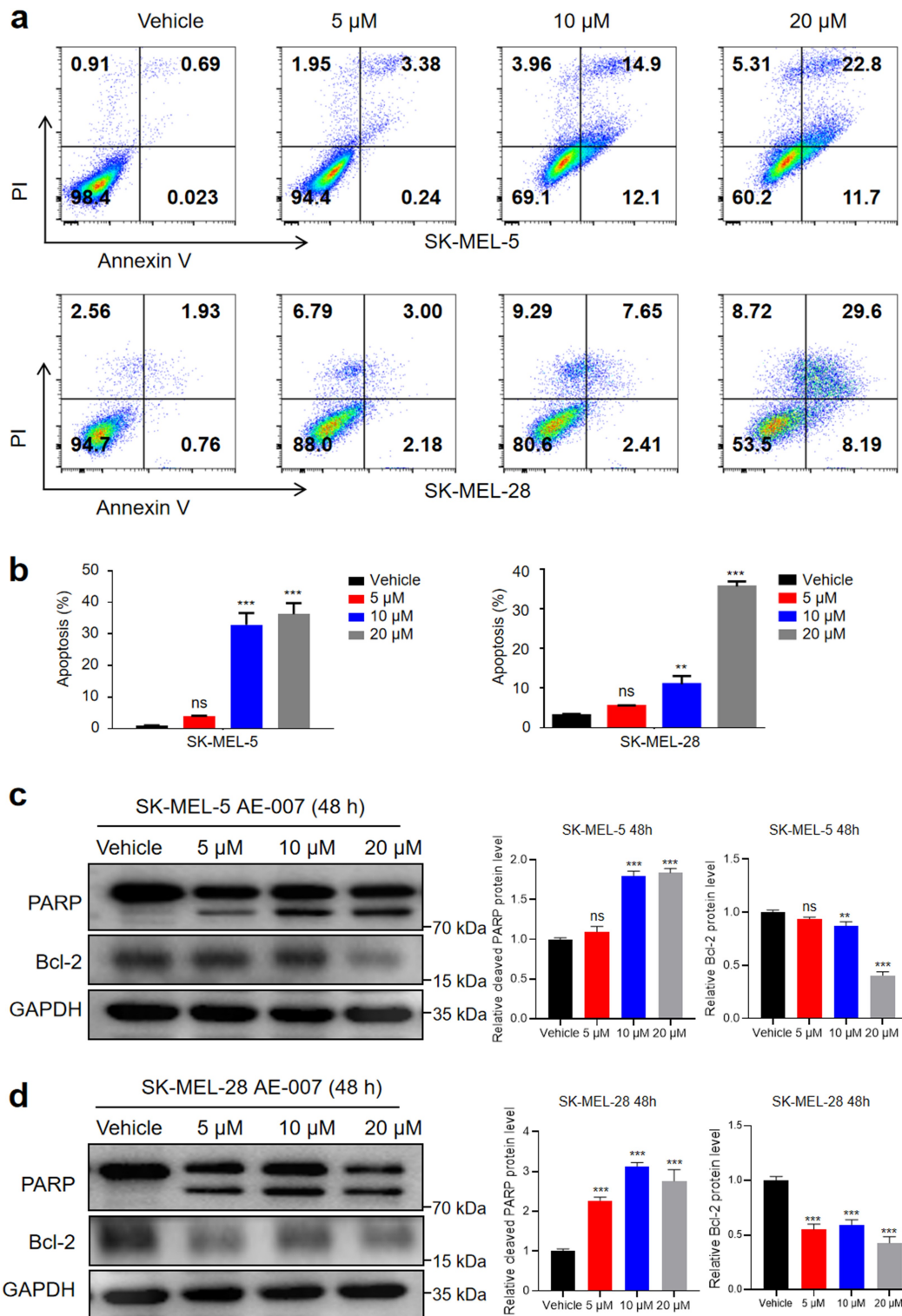


Figure 6. AE007 induces apoptosis in melanoma cells. **(a).** Apoptosis analysis of SK-MEL-5 (upper panel) and SK-MEL-28 (lower panel) cells treated with AE007 for 48 h. **(b).** Quantification of the cell apoptosis. **(c).** Western blot analysis of apoptosis-associated proteins in SK-MEL-5 cells treated with increasing concentrations of AE007 for 48 h. **(d).** Western blot analysis of apoptosis-associated proteins in SK-MEL-28 cells treated with increasing concentrations of AE007 for 48 h. One-way ANOVA analysis were performed in **b**, **c** and **d**. **, $P < 0.01$; ***, $P < 0.001$; ns, no significance.

in a mouse model. Consistently, mice treated with AE007 had significantly fewer and smaller metastatic nodules in their lungs, compared to those treated with vehicle (Figure 4e-f). Additionally, the mice in the AE007 treatment group had similar bodyweight to mice in the vehicle group (Figure 4f). These results demonstrated that AE007 inhibits melanoma cell invasion and migration.

AE007 induces cell cycle arrest and apoptosis in melanoma cells

To investigate the mechanism of AE007 inhibiting melanoma progression, SK-MEL-5 and SK-MEL-28 were treated with different concentrations of AE007 and the cell cycle were evaluated using flow cytometry. Results showed that AE007 increased the percentage of cell arrest in the G0/G1 phase (Figure 5a-b). Western blot analysis further validated the effects of AE007-induced cell cycle arrest, because AE007 treatment significantly reduced cyclin B1, cyclin D1, and CDK2 expression (Figure 5c-d). Moreover, flow cytometry analysis also demonstrated that AE007 increased the percentage of apoptotic cells in a dose-dependent manner (Figure 6a-b). Western blot analysis showed that AE007 increased the expression of the proapoptotic protein the cleavage of PARP in SK-MEL-5 and SK-MEL-28 cells, while it decreased the expression of the antiapoptotic protein Bcl-2 (Figure 6c-d). These finding suggested that AE007 arrests cell cycle progression and induces apoptosis in melanoma cells.

Transcriptomics identified a potential mechanism of AE007

To determine the molecular mechanism of AE007-mediated growth inhibition in melanoma cells, we analyzed global transcriptomic changes in melanoma cells treated with AE007. Bioinformatics analysis showed transcriptomic changes after AE007 treated for 24 h and 48 h (Figure 7a). With the relevant differentially expressed genes, the Kyoto Encyclopedia of Genes and Genomes (KEGG) approach was used. The top ten enriched pathways are related to cell proliferation. Therefore, AE007 may inhibit melanoma

proliferation by activating pathways associated with cell cycle, apoptosis, and DNA replication (Figure 7b). GSEA was then performed, and the cell cycle and DNA replication gene sets were found to be significantly inhibited after AE007 treatment (Figure 7c). Moreover, several key genes involved in cell cycle and DNA replication was quantified, such as growth arrest and DNA damage-inducible 45 alpha (GADD45A), SOX2 (Sex-determining region), CDKN1A (P21), and CCNB2 (Figure 7d). These results further validated our RNA-seq data, suggesting a potential mechanism for AE007 in melanoma.

Discussion

An RSK protein kinase is an enzyme that is activated by ERK1/2 and PDK1. They are activated by direct phosphorylation of Ser/Thr residues. RSK activity results in phosphorylation of cytoplasmic and nuclear RSK substrates, which contribute to cell growth and proliferation after their translocation [26]. Moreover, RSK2 is overexpressed and dysregulated in a variety of aggressive tumors, including melanoma [15], and it plays a substantial role in dealing with different type of cellular processes, including cell proliferation and transformation [27].

In this study, AE007 was identified by docking-based virtual screening (VS) and quantitative structure-activity relationship (QSAR) strategies to screen the SPECS database, and we next used cell-based inhibition and surface plasmon resonance (SPR) binding assays to verify the validity of the screening results [22]. And pull-down assay showed that AE007 directly binds to RSK2 and inhibits its protein kinase domain. Furthermore, we found that AE007 inhibited the proliferation, growth, and metastasis of melanoma cells in the indicated dose. AE007 displayed IC₅₀ values of 7.152 μ M, 7.079 μ M, and 9.050 μ M in A375, SK-MEL-5, and SK-MEL-28 cells, while IC₅₀ values of 27.870 μ M, and 20.510 μ M in PIG1 and HaCaT cells. This may be due to higher RSK2 expression in melanoma cells and lower RSK2 expression in PIG and HaCaT cells. AE007 also had inhibitory activity against melanoma xenografts in vivo, without obvious toxicity. Furthermore, western blot analysis revealed that RSK2 and its downstream

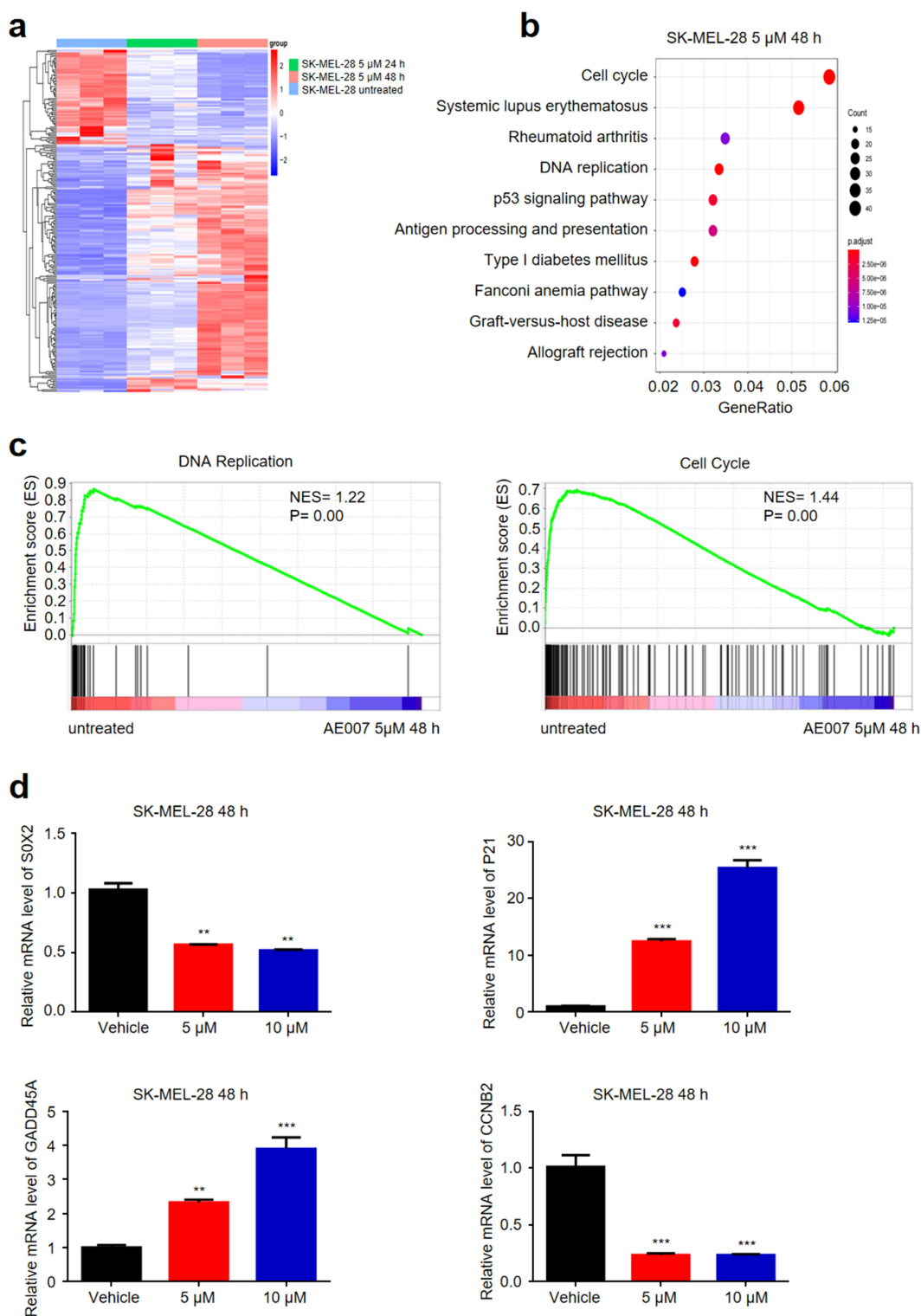


Figure 7. RNA-seq analysis showed the effect of AE007 on the gene expression profile. **(a)** Heatmap of gene expression in SK-MEL-28 cells after vehicle or AE007 treatment. **(b)** KEGG pathways with the highest enrichment after AE007 treatment. **(c)** GSEA indicating that DNA replication and cell cycle were significantly inhibited after AE007 treatment. **(d)** Gene expression of SOX2, P21, GADD45A, and CCNB2 in SK-MEL-28 cells after treatment with AE007 for 48 hours. One-way ANOVA analysis were performed in **b**. **, $P < 0.01$; ***, $P < 0.001$.

target p-CREB were decreased in melanoma cells after treatment with AE007. Therefore, the data highlights that AE007 appears to be a novel RSK2 inhibitor and offers a new treatment strategy for melanoma.

There are several RSK2 inhibitors targeting melanoma. For example, Aronchik et al. demonstrated that LJH685, a RSK2 inhibitor, potently and selectively inhibits RSK and the phosphorylation of its downstream YB1 to cause the inhibition of melanoma growth. Moreover, we previously identified another RSK2 inhibitor, CX-F9, which blocks melanoma cell proliferation and metastasis through autophagy. Additionally, Carnosol, a commercial inhibitor of RSK2, was shown to inhibit the progression of gastric cancer and melanoma. Carnosol is a phenolic diterpene isolated from *Rosmarinus officinalis* that has anticarcinogenic, anti-inflammatory, and antioxidant properties. Carnosol inhibits the invasion of B16/F10 mouse melanoma cells by suppressing metalloproteinase-9 through down-regulating nuclear factor-kappa B and c-Jun [21]. However, these RSK inhibitors reported over time, but none has been approved clinically owing to a number of issues, including the lack of appropriate pharmacokinetics and selectivity. Here, we identified AE007 as a novel inhibitor, which inhibit melanoma progression through inhibiting the phosphorylation of CREB. AE007 could be a promising melanoma therapeutic agent by targeting RSK2.

Our results demonstrate that AE007 targeting of the RSK2 NTKD induces both cell phase arrest and apoptosis. RSK2 regulates cell cycle regulators directly, promoting cell proliferation according to multiple lines of evidence. The transcription factor c-fos is known to regulate expression of cyclin D1 by affecting the stability of RSK2 [28]. Activating CDK is also facilitated by RSK2 through direct phosphorylation and activation of Cdc25c, an enzyme essential for activating the CDK/cyclin B complex [29]. Moreover, RSK2 inhibits FAS-induced apoptosis by phosphorylating caspase-8 [30]. The novel RSK2 inhibitor AE007 inhibits melanoma cells proliferation by inducing cell cycle arrest and apoptosis. RNA sequencing was used identification of genes and pathways that are involved in the potential molecular mechanisms by which AE007 inhibits melanoma cell proliferation. As a result of AE007 treatment,

GADD45A and P21 expression increased substantially, while CCNB2 expression raised. These are both cell cycle and apoptosis regulators. Apoptosis is the way to evaluate the therapeutic effect of drugs. Western blot analysis determined the molecular processes underlying the AE007-mediated pro-apoptotic effect in melanoma cells. PARP is activated after binding to DNA strand breaks; it is then cleaved, leading to apoptosis. Bcl-2, an apoptosis inhibitor, helps to suppress apoptosis in both benign and malignant tumors. The results suggest that AE007 enhances apoptosis through cleavage of PARP and downregulating Bcl-2 expression.

In conclusion, we identified a novel RSK2 inhibitor, AE007, by an in-silico screening approach. AE007 has antimelanoma activity and induces apoptosis and cell cycle arrest, resulting in new treatment strategy for melanoma. During the course of future experiments, studies will be conducted on the metabolism and clearance of the compound, its toxicity, and other related topics in order to determine its safety.

Conclusion

In summary, we identified a novel RSK2 inhibitor (AE007), which causes cell cycle arrest and cellular apoptosis, thereby dramatically inhibiting proliferation, migration and invasion of melanoma cells. Our findings will provide a strategy for the treatment of melanoma.

Acknowledgements

This study has benefited from substantial support and the efforts of all the stakeholders have been acknowledged for ensuring the success of this research. Particularly, it is important to acknowledge the support provided by Hunan province's Science and Technology Innovation Program (2021RC4013), National Natural Science Foundation of China. (Grant No. 81773341, 81974476, 82073458), 2020YFA0112904 from National Key Research and Development Project, Independent Exploration, and Innovation Project for Graduate students of Central South University (2020zzts872).

Disclosure statement

No potential conflict of interest was reported by the authors.

Funding

This work was supported by the National Natural Science Foundation of China, Grant No. 82073458 (Cong Peng), 81830096 (Xiang Chen), 8213000715 (Xiang Chen).

Author contributions

The research has relied on the contribution of a number of different authors providing input based upon their expertise in specific backgrounds. Yayun Li: conducted experiments, drafted the manuscript. Pian Yu: performed data acquisition, data analysis. Jing Long: contributed the compound. Ling Tang: performed data analysis. Xu Zhang: revised the manuscript. Zhe Zhou: revised the manuscript. Dongsheng Cao: Screened the compound. Juan Su: helped in data assessment and manuscript editing. Xiang Chen: supervised the projection and acquired the funding. Cong Peng: conceived the study and drafted the manuscript.

References

- Gordon R. Skin cancer: an overview of epidemiology and risk factors. *Semin Oncol Nurs.* 2013;29(3):160–169.
- Liu H, Kuang X, Zhang Y, et al. ADORA1 inhibition promotes tumor immune evasion by regulating the ATF3-PD-L1 axis. *Cancer Cell.* 2020;37(3):324–339 e8.
- Deng G, Zeng F, Su J, et al. BET inhibitor suppresses melanoma progression via the noncanonical NF-kappaB/SPP1 pathway. *Theranostics.* 2020;10(25):11428–11443.
- Farshidfar F, Rhrissorrakrai K, Levovitz C, et al. Integrative molecular and clinical profiling of acral melanoma links focal amplification of 22q11.21 to metastasis. *Nat Commun.* 2022;13(1):898.
- Degirmenci U, Wang M, Hu J. Targeting aberrant RAS/RAF/MEK/ERK signaling for cancer therapy. *Cells.* 2020;9(1):198.
- Arul N, Cho YY. A rising cancer prevention target of RSK2 in human skin cancer. *Front Oncol.* 2013;3:201.
- Yoo SM, Lee CJ, An HJ, et al. RSK2-Mediated ELK3 activation enhances cell transformation and breast cancer cell growth by regulation of c-fos promoter activity. *Int J Mol Sci.* 2019;20(8):1994.
- Cho YY, He Z, Zhang Y, et al. The p53 protein is a novel substrate of ribosomal S6 kinase 2 and a critical intermediary for ribosomal S6 kinase 2 and histone H3 interaction. *Cancer Res.* 2005;65(9):3596–3603.
- Linder M, Glitzner E, Srivatsa S, et al. EGFR is required for FOS-dependent bone tumor development via RSK2/CREB signaling. *EMBO Mol Med.* 2018;10(11). DOI:10.15252/emmm.201809408
- Yang X, Matsuda K, Bialek P, et al. ATF4 is a substrate of RSK2 and an essential regulator of osteoblast biology; implication for Coffin-Lowry syndrome. *Cell.* 2004;117(3):387–398.
- Cho YY, Yao K, Bode AM, et al. RSK2 mediates muscle cell differentiation through regulation of NFAT3. *J Biol Chem.* 2007;282(11):8380–8392.
- Li LY, Chen XS, Wang KS, et al. RSK2 protects human breast cancer cells under endoplasmic reticulum stress through activating AMPKalpha2-mediated autophagy. *Oncogene.* 2020;39(43):6704–6718.
- Ma J, Lu Y, Zhang S, et al. beta-Trcp ubiquitin ligase and RSK2 kinase-mediated degradation of FOXN2 promotes tumorigenesis and radioresistance in lung cancer. *Cell Death Differ.* 2018;25(8):1473–1485.
- Clark DE, Errington TM, Smith JA, et al. The serine/threonine protein kinase, p90 ribosomal S6 kinase, is an important regulator of prostate cancer cell proliferation. *Cancer Res.* 2005;65(8):3108–3116.
- Cho YY, Lee MH, Lee CJ, et al. RSK2 as a key regulator in human skin cancer. *Carcinogenesis.* 2012;33(12):2529–2537.
- Smith JA, Poteet-Smith CE, Xu Y, et al. Identification of the first specific inhibitor of p90 ribosomal S6 kinase (RSK) reveals an unexpected role for RSK in cancer cell proliferation. *Cancer Res.* 2005;65(3):1027–1034.
- Sapkota GP, Cummings L, Newell FS, et al. BI-D1870 is a specific inhibitor of the p90 RSK (ribosomal S6 kinase) isoforms in vitro and in vivo. *Biochem J.* 2007;401(1):29–38.
- Han JH, Kim S, Kim S, et al. FMK, an inhibitor of p90RSK, inhibits high glucose-induced TXNIP expression via regulation of ChREBP in pancreatic beta cells. *Int J Mol Sci.* 2019;20(18):4424.
- Aronchik I, Appleton BA, Basham SE, et al. Novel potent and selective inhibitors of p90 ribosomal S6 kinase reveal the heterogeneity of RSK function in MAPK-driven cancers. *Mol Cancer Res.* 2014;12(5):803–812.
- Wang L, Zhang Y, Liu K, et al. Carnosol suppresses patient-derived gastric tumor growth by targeting RSK2. *Oncotarget.* 2018;9(76):34200–34212.
- Huang SC, Ho CT, Lin-Shiau SY, et al. Carnosol inhibits the invasion of B16/F10 mouse melanoma cells by suppressing metalloproteinase-9 through down-regulating nuclear factor-kappa B and c-Jun. *Biochem Pharmacol.* 2005;69(2):221–232.
- Yue Z, Rfc A, Zkd B, et al. Discovery of novel p90 ribosomal S6 kinase 2 inhibitors for potential cancer treatment through ligand-based and structure-based virtual screening methods. *Chemometrics and Intelligent Laboratory Systems.* 2021;217:104402.
- Zhang X, Cai L, Zhao S, et al. Corrigendum to “CX-F9, a novel RSK2 inhibitor, suppresses cutaneous melanoma cells proliferation and metastasis through regulating autophagy” [Biochem. Pharmacol. 168 (2019), 14–25]. *Biochem Pharmacol.* 2021;184:114372.

- [24] Lian C, Cao S, Zeng W, et al. RJT-101, a novel camptothecin derivative, is highly effective in the treatment of melanoma through DNA damage by targeting topoisomerase 1. *Biochem Pharmacol.* [2020](#);171:113716.
- [25] Liu N, Wang KS, Qi M, et al. Vitexin compound 1, a novel extraction from a Chinese herb, suppresses melanoma cell growth through DNA damage by increasing ROS levels. *J Exp Clin Cancer Res.* [2018](#);37(1):269.
- [26] Houles T, Roux PP. Defining the role of the RSK isoforms in cancer. *Semin Cancer Biol.* [2018](#);48:53–61.
- [27] Schaeffer HJ, Weber MJ. Mitogen-activated protein kinases: specific messages from ubiquitous messengers. *Mol Cell Biol.* [1999](#);19(4):2435–2444.
- [28] Murphy LO, Smith S, Chen RH, et al. Molecular interpretation of ERK signal duration by immediate early gene products. *Nat Cell Biol.* [2002](#);4(8):556–564.
- [29] Wang R, Jung SY, Wu CF, et al. Direct roles of the signaling kinase RSK2 in Cdc25C activation during *Xenopus* oocyte maturation. *Proc Natl Acad Sci USA.* [2010](#);107(46):19885–19890.
- [30] Peng C, Cho YY, Zhu F, et al. Phosphorylation of caspase-8 (Thr-263) by ribosomal S6 kinase 2 (RSK2) mediates caspase-8 ubiquitination and stability. *J Biol Chem.* [2011](#);286(9):6946–6954.